Available online at http://scik.org

J. Math. Comput. Sci. 11 (2021), No. 2, 1486-1498

https://doi.org/10.28919/jmcs/5401

ISSN: 1927-5307

A STUDY OF NON-ISOTHERMAL PERMEABLE FLOW OF NANO-FLUIDS IN A STRETCHABLE ROTATING DISK SYSTEM

A. O. AKINDELE*, A. W. OGUNSOLA

Department of Pure and Applied Mathematics, Ladoke Akintola University of Technology, Ogbomoso, Nigeria

Abstract: The rapid development of modern nanotechnology has brought about the importance of particles of nanometer-size (normally less than 100 nm) as compared to those of macro meter-size. Occurrences of heat transfer in flow of nanofluids are more prominent in industries and advanced technological processes. Transportation, atomic reactors, lubricating system and polymer processing are few of such processes. A non-isothermal permeable flow of nanofluids between dual stretching and rotating disks was examined. The governing nonlinear conservation equations were considered in cylindrical coordinate and Von Karman transformations were rendered into the system, the emerging boundary value problem was associated with a number of dimensionless parameters, such as, Prandtl number, upper and lower disk stretching parameters, permeability and relative rotation rate parameters. The Nano- fluid model was used to account for the effects of Brownian and Thermophoresis motion on the flow system. The resulting nonlinear system of equations is then solved using Newton's Finite difference technique by MAPLE 18.0 software. The numerical solution obtained showed the effects of the associated physical parameters on the velocities, temperature, pressure and the concentration profiles presented graphically.

Keywords: nanoparticles; porous medium; non-isothermal flow; Brownian motion; thermophoresis motion; relative rotation; stretchable rotating disks.

2010 AMS Subject Classification: 58D30, 80A20, 65C20.

*Corresponding author

E-mail address: aoakindele65@pgshcool.lautech.edu.ng

Received January 8, 2021

1. INTRODUCTION

The Study of nanometer-sized particles diffused into base fluids has received considerable and appreciable attentions in the last few decades due to its various industrial and biological applications. These applications are evident in chromatography, pollutant migration, design of toxic waste storage, flows in proximal tube, regenerative heat exchangers, raw petroleum generation, gaseous diffusion in binary mixtures, crystal growing, electronic chips, filaments and wires, glass blowing, cooling of metallic sheet, artificial fibers, paper production, metallurgical processes, tinning of copper wires and many other industrial applications as can be found in Pop and Ingham [1] and Vafai [2].

In the past effort to analyzed fluid with nanoparticles, Sobamowo *et al*. [3] presented thermo-magneto-solutal squeezing flow of nanofluid between two parallel disks embedded in a porous medium: effects of nanoparticles geometry slip and temperature jump conditions were reported. Sravan and Rushi [4] examine the effect of homogeneous-heterogeneous reactions in MHD stagnation point nanofluid flow toward a cylinder with nonuniform heat source or sink. Hayat *et al.* [5] studied the unsteady flow of nanofluid through porous medium with variable characteristics. In the recent past, Dianchen *et al.* [6] considered the analysis of unsteady flow and heat transfer of nanofluid using Blasius-Rayleigh-Stokes variable. The numerical study of heat transfer and viscous flow in a dual rotating extendable disk system with a non-Fourier heat flux model was explored by Shamshuddin *et al.* [7]. Hayat *et al.* [8] considerd a flow between two stretchable rotating disks with Cattaneo-Christov heat flux model.Recent progress about nanofluid can be mentioned through refs [9-20]. Hsiao [21] studied conjugate mixed convective flow of nanofluid with radiation. Abubakar *et al.* [22] examined the stability analysis on the flow and heat transfer of nanofluid past a stretching/shrinking cylinder with suction effect. Fang and Zhang [23] reported the flow between two stretchable disks with exact solution of Navier-Stokes equations.

The objective of the present study is to analyze the development of the steady flow of nanofluid in a cylindrical coordinate. The velocities profiles, pressure profile, thermal field and the concentration profile are taken into consideration. The system of governing non-linear partial differential equations was transformed into their ordinary differential equations equivalents and

the resulting equations were solved numerically by Newton's Finite difference technique subjected to appropriate boundary conditions.

2. MATHEMATICAL FORMULATION

Following [7], the flow in the gap between two stretchable rotating disks in cylindrical coordinate systems (r, θ, z) was considered. The gap contains a high permeability porous medium, nanofluid and Darcy's law is valid. The upper and the lower disks are separated by distance h. The two disks rotate in an anticlockwise direction with rotational velocities Ω_1 and Ω_2. The disks are deformable and a_1 (lower) and a_2 (upper) are their stretching rates. Forced convection takes place between the two disks and the upper disk is maintained at temperature T_2 and the lower disk at lesser temperature of T_1. The flow geometry is as shown on figure 1. The conservation equation for mass (continuity), radial, tangential and axial momentum, energy conservations and concentration equation models are as follows:

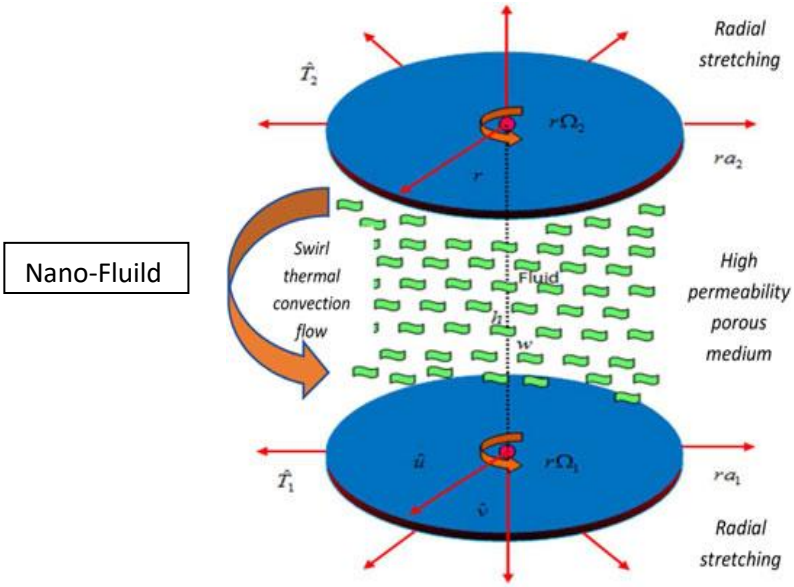

Figure 1: permeable flow geometry between two rotating disks

Nomenclature

(r, θ, z): Cylindrical coordinate
a_1: Lower stretching rate
a_2: Upper stretching rate
A: Pressure parameter
A_1, A_2: Scaled stretching parameter
C: Concentration (kg/m^3)
C_1: Concentration at the lower disk (kg/m^3)
C_2: Concentration at the upper disk (kg/m^3)
C_p: Specific heat at constant pressure (J/kg K)
D_B: Brownian motion coefficient (m^2/s)
D_T: Thermophoretic diffusion coefficient (m^2/s)
f: Radial velocity profile
g: Tangential velocity profile
h: Distance between the disks
k: Thermal conductivity
k_0: permeability constant
Le: Lewis number
N_b: Brownian motion parameter
N_t: Thermoporesis parameter
P: Pressure (N/m^2)
Pr : Prandtl's number
Re: Local Reynolds number
t: Time
T: Fluid temperature
T_1: Temperature at the lower disk
T_2: Temperature at the upper disk
T_∞ : Ambient temperature
u: Radial velocity
v: Tangential velocity
w: Axial velocity

Greek symbols
η : Similarity variable
ν: Kinematic viscosity
β : Permeable parameter
μ : Dynamic viscosity
ψ: Stream function
ρ : Density
σ: Thermal diffusivity of the fluid
ε: Ratio of the heat capacities of the nanoparticles
θ: Dimensionless temperature variable
Ω_1: Lower rotational velocity
Ω_2: Upper rotational velosity
τ: Relative rotational parameter
ϕ: Dimensionless nanoconcentration parameter
$\boldsymbol{\nu}_f$: Fluid viscosity

$$\frac{\partial u}{\partial r}+\frac{u}{r}+\frac{\partial w}{\partial z}=0 \tag{1}$$

$$u\frac{\partial u}{\partial r}+w\frac{\partial u}{\partial z}-\frac{v^2}{r}=-\frac{1}{\rho}\frac{\partial p}{\partial r}+\nu\left(\frac{\partial^2 u}{\partial r^2}+\frac{1}{r}\frac{\partial u}{\partial r}+\frac{\partial^2 u}{\partial z^2}-\frac{u}{r^2}\right)-\frac{\mu}{k_0}u \tag{2}$$

$$u\frac{\partial v}{\partial r}+w\frac{\partial v}{\partial z}+\frac{uv}{r}=\nu\left(\frac{\partial^2 v}{\partial r^2}+\frac{1}{r}\frac{\partial v}{\partial r}+\frac{\partial^2 v}{\partial z^2}-\frac{v}{r^2}\right)-\frac{\mu}{k_0}v \tag{3}$$

$$w\frac{\partial w}{\partial z}+u\frac{\partial w}{\partial r}=-\frac{1}{\rho}\frac{\partial p}{\partial z}+\nu\left(\frac{\partial^2 w}{\partial r^2}+\frac{1}{r}\frac{\partial w}{\partial r}+\frac{\partial^2 w}{\partial z^2}\right)-\frac{\mu}{k_0}w \tag{4}$$

$$u\frac{\partial T}{\partial r}+w\frac{\partial T}{\partial z}=\frac{k}{\rho C_p}\left(\frac{\partial^2 T}{\partial r^2}+\frac{\partial^2 T}{\partial z^2}+\frac{1}{r}\frac{\partial T}{\partial r}\right)+\frac{\varepsilon\nu}{\sigma}\left(D_B\frac{\partial T}{\partial z}\frac{\partial C}{\partial z}+\frac{D_T}{T_\infty}\left(\frac{\partial T}{\partial z}\right)^2\right) \tag{5}$$

$$u\frac{\partial C}{\partial r}+w\frac{\partial C}{\partial z}=D_B\left(\frac{\partial^2 C}{\partial r^2}+\frac{1}{r}\cdot\frac{\partial C}{\partial r}+\frac{\partial^2 C}{\partial z^2}\right)+\frac{D_T}{T_\infty}\left(\frac{\partial^2 T}{\partial r^2}+\frac{1}{r}\cdot\frac{\partial T}{\partial r}+\frac{\partial^2 T}{\partial z^2}\right) \tag{6}$$

with initial and boundary conditions

$$\left.\begin{array}{ll} u = ra_1,\ v = r\Omega_1,\ w = 0,\ T = T_1,\ C = C_1 & \text{at } z = 0 \quad \text{(disk1)} \\ u = ra_2,\ v = r\Omega_2,\ w = 0,\ T = T_2,\ C = C_2 & \text{at } z = h \quad \text{(disk 2)} \end{array}\right\} \tag{7}$$

2. SIMILARITY TRANSFORMATIONS

Following Fang and Zhang, the Von Karman similarity transformation is invoked using:

$$\left.\begin{array}{l} u = r\Omega_1 f'(\eta),\ v = r\Omega_1 g(\eta),\ w = -2h\Omega_1 f(\eta),\quad \eta=\dfrac{z}{h} \\ \theta(\eta)=\dfrac{T-T_2}{T_1-T_2} \qquad P=\rho_f\Omega_1\nu_f\left(P(\eta)+\dfrac{1}{2}\dfrac{r^2}{h^2}A\right) \quad \phi(\eta)=\dfrac{C-C_2}{C_1-C_2} \end{array}\right\} \tag{8}$$

where, u, v, w are the radial, tangential, and axial velocity components in the (r, θ, z) directions respectively. T is the temperature, ν is the kinematic viscosity, p is hydrodynamic pressure of the fluid and ρ is the density of the fluid.

The mass conservation law equation (1) is identically satisfied. However, the radial, tangential and axial momentum equations (replaced with the pressure equation), the energy and the concentration equations are reduced to the equivalent nonlinear coupled system of ordinary differential equations:

$$f''' + \mathrm{Re}(2ff'' - f'^2 + g^2 - \frac{1}{\beta} f') - A = 0 \quad (9)$$

$$\mathrm{Re}(2f'g - 2fg' + \frac{1}{\beta} g) - g'' = 0 \quad (10)$$

$$p' = \mathrm{Re}(\frac{2}{\beta} f - 4ff') - 2f'' \quad (11)$$

$$\theta'' + 2\,\mathrm{Pr}\,\mathrm{Re}\, f\theta' + \mathrm{Pr}(N_b\theta'\varphi' + N_t\theta'^2) = 0 \quad (12)$$

$$\varphi'' + \frac{N_t}{N_b}\theta'' + 2\,\mathrm{Re}\,Le\cdot f\varphi' = 0 \quad (13)$$

The corresponding boundary conditions (7) at lower and upper disk transform to:

$$\left.\begin{array}{l} \text{Lower disk: } f(0) = 0,\ f'(0) = A_1, g(0) = 1, P(0) = 0, \theta(0) = 1, \varphi(0) = 1 \\ \text{Upper disk: } f'(1) = A_2, g(1) = \tau, \theta(1) = 0, \varphi(1) = 0 \end{array}\right\} \quad (14)$$

where Re denotes Reynolds number, Pr prandtl number, A_1 and A_2 are scaled stretching parameters,τ rotation number, β porosity parameter, Le is lewis number, N_t the thermophoresis parameter and N_b Brownian motion parameter, and then:

$$\left.\begin{array}{l} \mathrm{Re} = \dfrac{h^2\Omega_1}{\nu}, \beta = \dfrac{k_0\Omega_1}{\nu}, Le = \dfrac{\nu}{D_B}, \mathrm{Pr} = \dfrac{\rho c_p \nu}{k}, N_b = \dfrac{\varepsilon D_B (C_1 - C_2)}{\sigma}, \\ N_t = \dfrac{\varepsilon D_T (T_1 - T_2)}{T_\infty \sigma}, \tau = \dfrac{\Omega_2}{\Omega_1}, A_1 = \dfrac{a_1}{\Omega_1}, A_2 = \dfrac{a_2}{\Omega_2}. \end{array}\right\} \quad (15)$$

3. NUMERICAL SOLUTION

Equations (9) to (13) along with the associated boundary conditions (14) were solved numerically via Newton's finite difference method with the help of Maple 18.0 software. In this method, the system of ODEs is converted to a first-order system by introducing a new dependent variable then the derivatives are replaced by finite-difference approximations, to form a system of algebraic equations; a mesh of evenly spaced points is then defined on the solution interval and the algebraic equations are solved at the mesh points by Newton's iteration scheme.

The solution depend on Brownian parameter (Nb), thermophoresis parameter (Nt), pressure constant (A), Reynolds number (Re), relative rotational parameter (τ), Lewis number (Le), Prandtl number (Pr) and scaled stretching parameter (A_1). The effects of parameters were discussed and graphical results were presented to explore stimulating aspects of the parameters on related profiles.

4. RESULTS AND DISCUSSION

In the investigation we analyze the permeable flow of nanofluid in a stretchable rotation disk system, the effect of flow parameters were obtained from the solution. The purpose of this section is to interpret the graphical description of sundry variables such as local Reynolds number (Re), Prandtl number (Pr), pressure constant (A), Lewis number (Le), Brownian motion parameter (N_b), Thermophoresis parameter (N_t), relative rotational parameter (τ) and scaled stretching parameter (A_1) on radial velocities f (η) and $f'(\eta)$, tangential velocity $g(\eta)$, Pressure profile P (η), thermal field θ (η) and the concentration field φ (η). Figure.2 elaborates the characteristics of Reynolds number (Re) on f (η). Here radial velocities f (η) is higher for (Re). Behavior of Reynolds number (Re) on $f'(\eta)$ is addressed in figure.3. Higher (Re) yields more radial velocity $f'(\eta)$. Figure.4 and figure.5 highlighted the impacts of pressure constant (A) on f (η) and $f'(\eta)$ respectively. It is that f (η) and $f'(\eta)$ possesses opposite trend on the pressure constant (A). Figure.6 and figure.7 witnessed that scaled stretching parameter (A_1) increases the velocities $f(\eta)$ and $f'(\eta)$ respectively. Figure.8 is sketched to scrutinize the behavior of $g(\eta)$ through (Re). an enhancement in $g(\eta)$ is observed through lower (Re). Plot of $g(\eta)$ against relative rotational parameter (τ) is illustration in figure.9, clearly $g(\eta)$ is enhanced for higher (τ). Figure.10 elaborate the role of (Re) on P (η). It shows an increment in (Re) leads to a decrement in the pressure profile but later increase the pressure profile. Attributes of P (η) against (A_1) is presented in figure.11, higher P (η) is observed by increasing (A_1). Figure.12 analyzed that higher estimation of (Re) lowers the thermal field θ (η). Figure.13 displayed behavior of thermal field θ (η) against prandtl number (Pr). Clearly higher estimation of (Pr) increases the thermal field θ (η).

Figure.14 displayed the behavior of (N_t) on the thermal field θ (η). Higher (N_t) leads to stronger θ (η). Role of (Re) on φ (η) is elaborated in figure.15. Here concentration φ (η) is a increasing function of (Re). Characteristics of (Pr) and (Le) on concentration profile φ (η) are portrayed in figure.16 and figure.17. opposite trend on φ (η) is noted through (Pr) and (Le). Figure.18 sketched the attributes of φ (η) for (N_t). Reduction in φ (η) is seen through higher (N_t). Outcome

of (N_b) on the concentration profile φ (η) is plotted in figure.19. clearly higher (N_b) strengthen the concentration field φ (η).

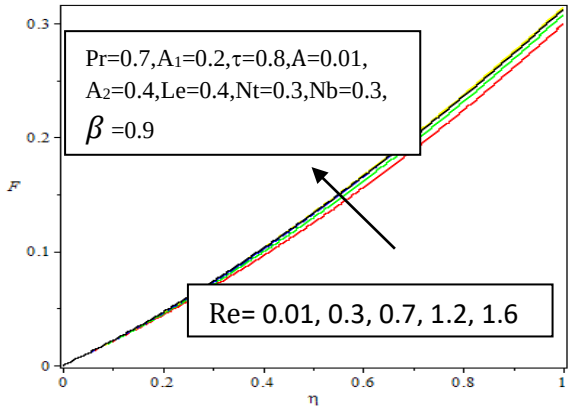

. Fig.2. Graph of f (η) for various Re.

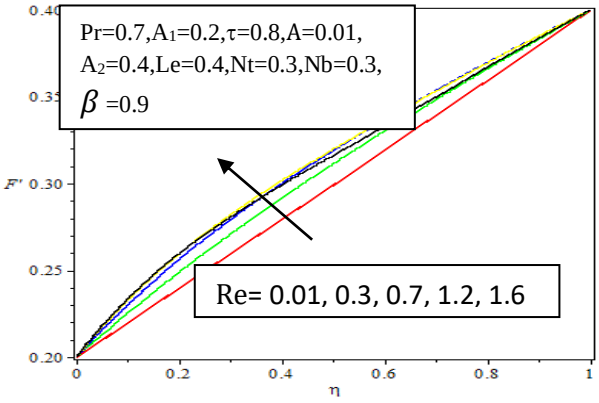

Fig. 3. Graph of f ' (η) for various Re.

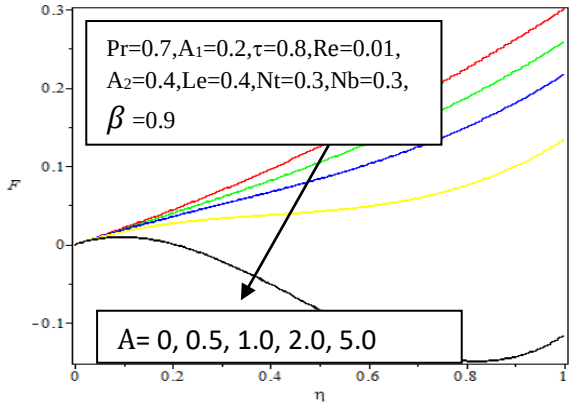

Fig. 4. Graph of f (η) for various A.

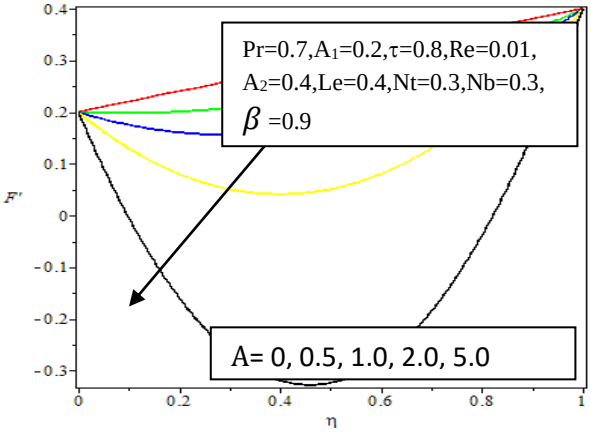

Fig. 5. Graph of f ' (η) for various A.

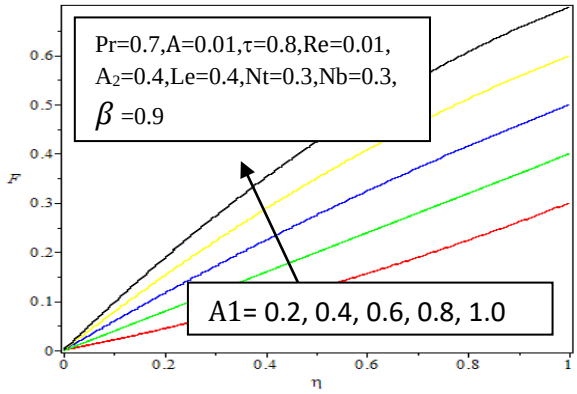

Fig. 6. Graph of f (η) for various A1.

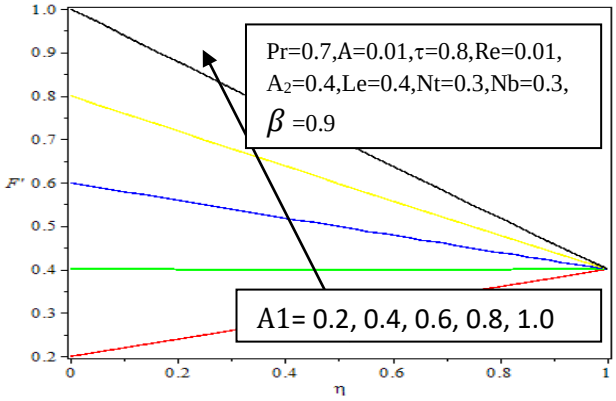

Fig. 7. Graph of f ' (η) for various A1.

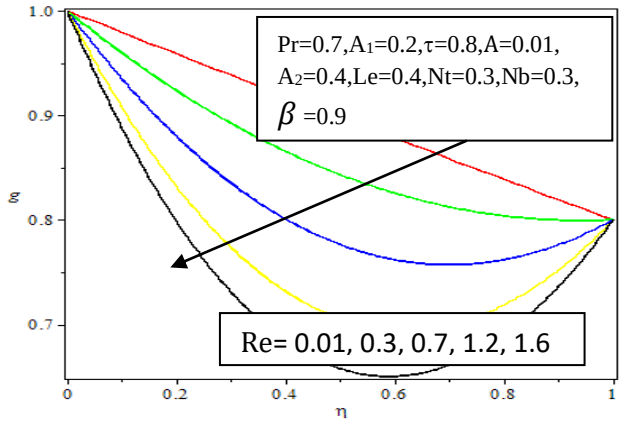

Fig. 8. Graph of g (η) for various Re.

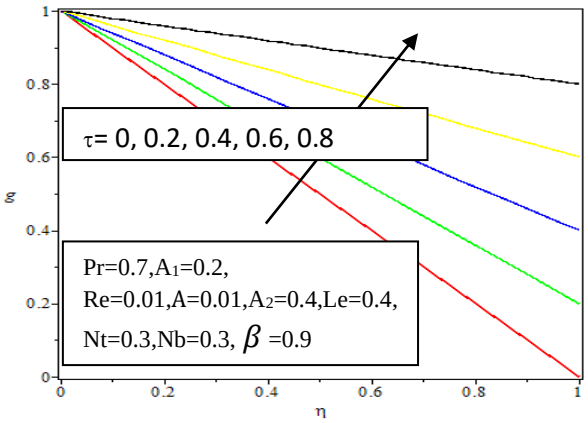

Fig. 9. Graph of g (η) for various τ.

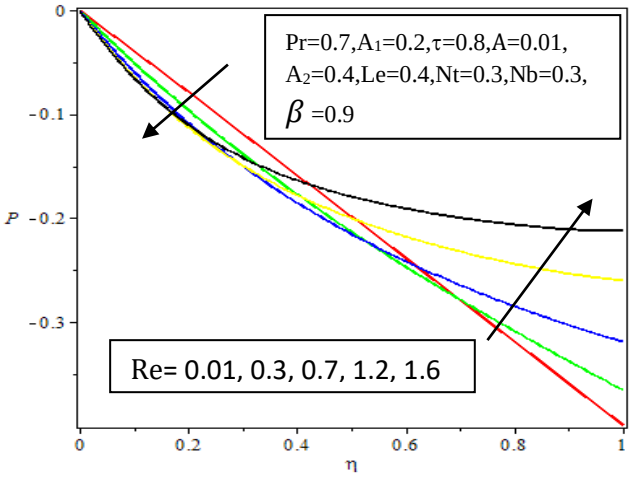

Fig. 10. Graph of P (η) for various Re.

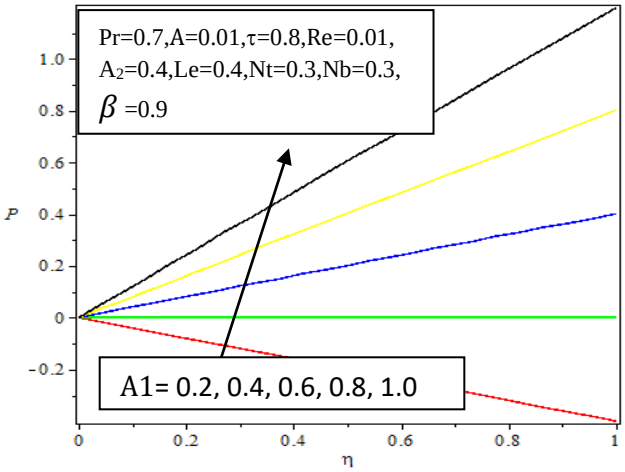

Fig. 11. Graph of P (η) for various A1.

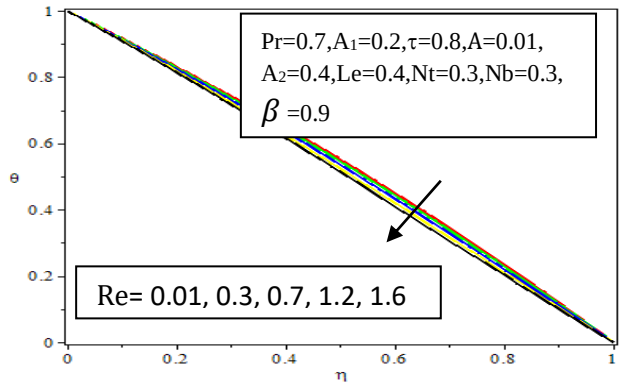

Fig. 12. Graph of θ (η) for various Re.

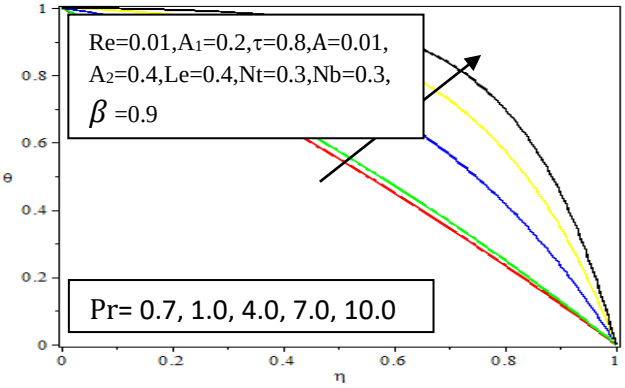

Fig. 13. Graph of θ (η) for various Pr.

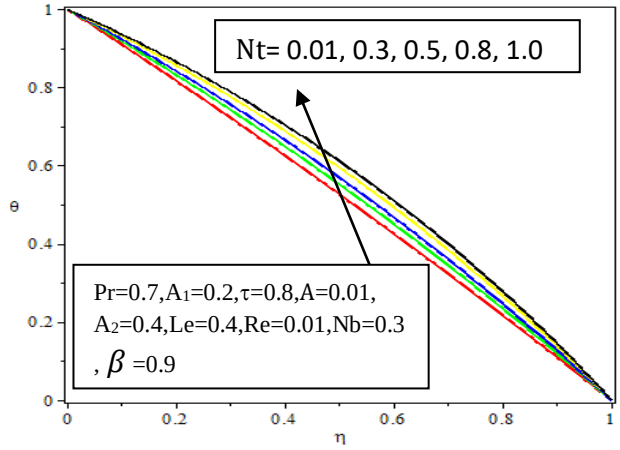

Fig. 14. Graph of θ (η) for various Nt

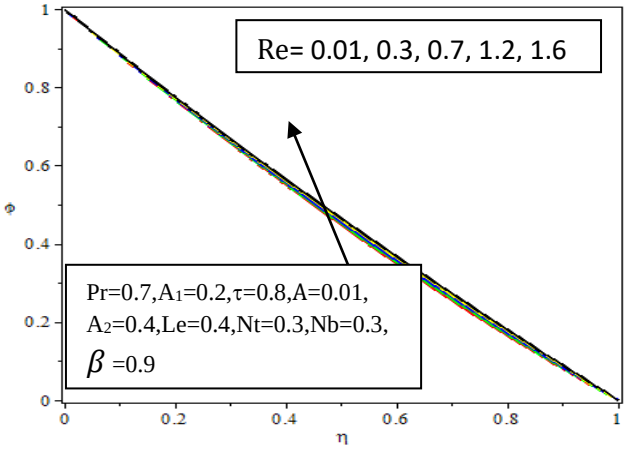

Fig. 15. Graph of φ (η) for various Re.

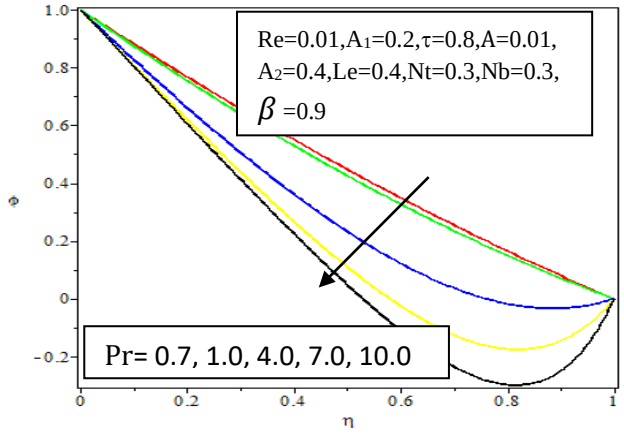

Fig. 16. Graph of φ (η) for various Pr.

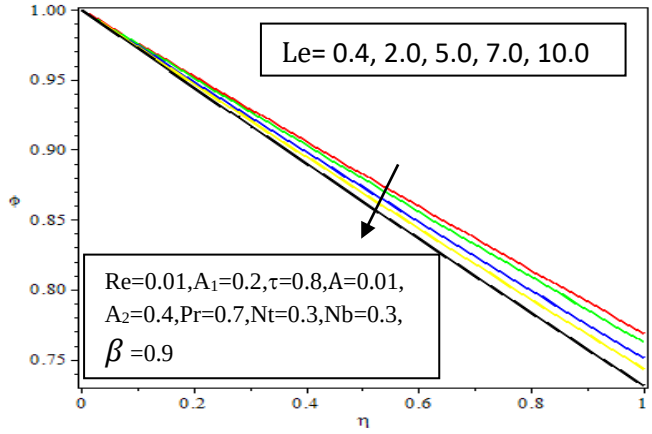

Fig. 17. Graph of φ (η) for various Le.

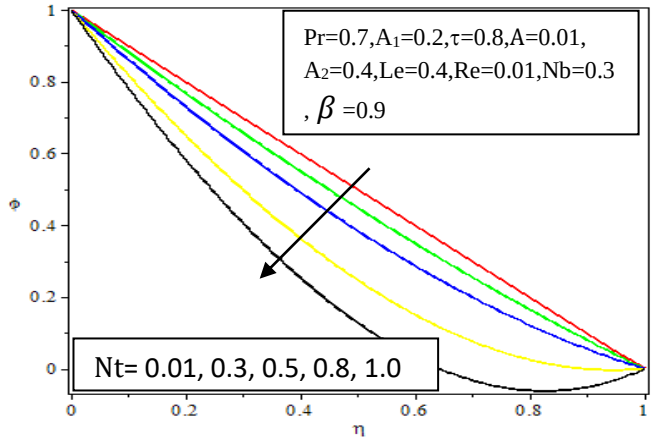

Fig. 18. Graph of φ (η) for various Nt.

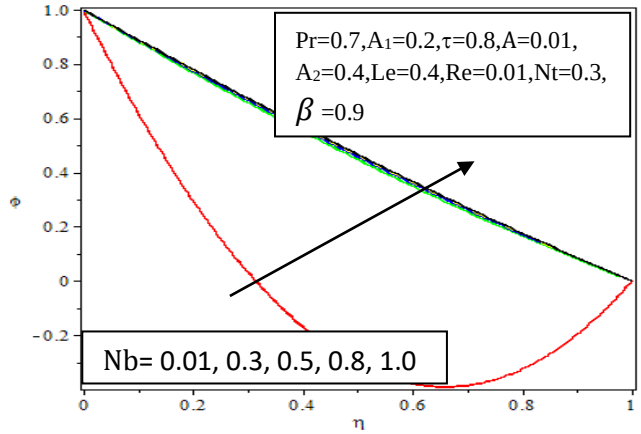

Fig. 19. Graph of φ (η) for various Nb.

5. CONCLUSION

In this paper, the effect of Brownian motion parameter, thermophoresis parameter and scaled stretching parameter on a permeable flow between two rotating disks have been investigated analytically using the Newton's difference method. Also, the influence of various flow parameters such as Lewis number, Prandtl number, Reynolds number, pressure constant and relative rotational parameter on the radial and tangential velocities, Pressure profile, thermal field and the concentration profile were investigated. It is established in the study that the addition of nanoparticles to the base fluid enhances its thermal conductivity. Base on the study, the following remarks were made.

1) As the Reynolds number increases, the radial velocity component and the concentration profile increases significantly while the tangential velocity component and the thermal field decreases. For the Pressure profile, it first experiences a deceleration but later accelerate at some point.
2) The radial velocity component and the Pressure profile increases with an increase in the scaled stretching parameter.
3) As the Thermophoresis parameter increases, the thermal field increases. A reverse case is recorded on the concentration profile.
4) Increasing the Brownian motion parameter evokes a corresponding increase in the concentration distribution and also, increasing the Lewis number, retardation occurs on the concentration profile.
5) Increasing the value of the Prandtl number, the concentration distribution decreases significantly, while accelerate rapidly on the thermal field.

CONFLICT OF INTERESTS

The author(s) declare that there is no conflict of interests.

REFERENCES

[1] Pop, D.B. Ingham, (eds.) Convective heat transfer: Mathematical and computational modelling of viscous fluids and porous media. Pergamon, Oxford (2001).

[2] K. Vafai, Porous Media: Applications in Biological Systems and Biotechnology. CRC Press, Tokyo (2010).

[3] M.G. Sobamowo, A.T. Akinshilo, A.A. Yinusa, Thermo-Magneto-Solutal Squeezing Flow of Nanofluid between Two Parallel Disks Embedded in a Porous Medium: Effects of Nanoparticle Geometry, Slip and Temperature Jump Conditions, Model. Simul. Eng. 2018 (2018), 7364634.

[4] T. Sravan Kumar, B. Rushi Kumar, Effect of Homogeneous-Heterogeneous Reactions in MHD Stagnation Point Nanofluid Flow Toward a Cylinder with Nonuniform Heat Source or Sink, in: B. Rushi Kumar, R. Sivaraj, B.S.R.V. Prasad, M. Nalliah, A.S. Reddy (Eds.), Applied Mathematics and Scientific Computing, Springer International Publishing, Cham, 2019: pp. 287–299.

[5] T. Hayat, F. Haider, A. Alsaedi, B. Ahmad, Unsteady flow of nanofluid through porous medium with variable characteristics, Int. Commun. Heat Mass Transfer. 119 (2020), 104904.

[6] D. Lu, S. Mumtaz, U. Farooq, A. Ahmad, Analysis of Unsteady Flow and Heat Transfer of Nanofluid Using Blasius–Rayleigh–Stokes Variable, Coatings. 9 (2019), 211.

[7] M. Shamshuddin, S.R. Mishra, O.A. Bég, A. Kadir, Numerical study of heat transfer and viscous flow in a dual rotating extendable disk system with a non-Fourier heat flux model, Heat Transfer-Asian Res. 48 (2019), 435–459.

[8] T. Hayat, S. Qayyum, M. Imtiaz, A. Alsaedi, Flow between two stretchable rotating disks with Cattaneo-Christov heat flux model, Results Phys. 7 (2017), 126–133.

[9] M. Turkyilmazoglu, Bödewadt flow and heat transfer over a stretching stationary disk, Int. J. Mech. Sci. 90 (2015), 246–250.

[10] N. Shehzad, A. Zeeshan, R. Ellahi, K. Vafai, Convective heat transfer of nanofluid in a wavy channel: Buongiorno's mathematical model, J. Mol. Liquids. 222 (2016), 446–455.

[11] B. Mahanthesh, F. Mabood, B.J. Gireesha, R.S.R. Gorla, Effects of chemical reaction and partial slip on the three-dimensional flow of a nanofluid impinging on an exponentially stretching surface, Eur. Phys. J. Plus. 132 (2017), 113.

[12] K. Ganesh Kumar, G.K. Ramesh, B.J. Gireesha, R.S.R. Gorla, Characteristics of Joule heating and viscous dissipation on three-dimensional flow of Oldroyd B nanofluid with thermal radiation, Alexandria Eng. J. 57 (2018), 2139–2149.

[13] W. Jiang, G. Chen, Dispersion of active particles in confined unidirectional flows, J. Fluid Mech. 877 (2019), 1–34.

[14] H. Xu, Modelling unsteady mixed convection of a nanofluid suspended with multiple kinds of nanoparticles between two rotating disks by generalized hybrid model, Int. Commun. Heat Mass Transfer. 108 (2019), 104275.

[15] M. Alghamdi, Significance of Arrhenius Activation Energy and Binary Chemical Reaction in Mixed Convection Flow of Nanofluid Due to a Rotating Disk, Coatings. 10 (2020), 86.

[16] W. Jiang, G. Chen, Dispersion of gyrotactic micro-organisms in pipe flows, J. Fluid Mech. 889 (2020), A18.

[17] T. Rafiq, M. Mustafa, Computational Analysis of Unsteady Swirling Flow Around a Decelerating Rotating Porous Disk in Nanofluid, Arab. J. Sci. Eng. 45 (2020), 1143–1154.

[18] M. Turkyilmazoglu, Single phase nanofluids in fluid mechanics and their hydrodynamic linear stability analysis, Computer Meth. Programs Biomed. 187 (2020), 105171.

[19] M.A. Sadiq, Serious Solutions for Unsteady Axisymmetric Flow over a Rotating Stretchable Disk with Deceleration, Symmetry. 12 (2020), 96.

[20] M.D.K. Niazi, H. Xu, Modelling two-layer nanofluid flow in a micro-channel with electro-osmotic effects by means of Buongiorno's mode, Appl. Math. Mech.-Engl. Ed. 41 (2020), 83–104.

[21] K.-L. Hsiao, Nanofluid flow with multimedia physical features for conjugate mixed convection and radiation, Computers Fluids. 104 (2014), 1–8.

[22] N.A.A. Bakar, N. Bachok, N.Md. Arifin, I. Pop, Stability analysis on the flow and heat transfer of nanofluid past a stretching/shrinking cylinder with suction effect, Results Phys. 9 (2018), 1335–1344.

[23] T. Fang, J. Zhang, Flow between two stretchable disks—An exact solution of the Navier–Stokes equations, Int. Commun. Heat Mass Transfer. 35 (2008), 892–895.